Predicting Frictional Properties of Graphene Kirigami Using Molecular Dynamics and Neural Networks

Designs for a negative friction coefficient

Mikkel Metzsch Jensen

University of Oslo

Juni 02, 2023

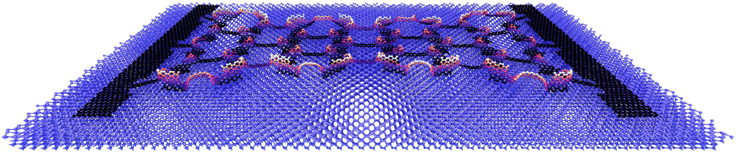

Outline

Thesis overview

1. **Sheet modification**: Alter a graphene sheet using atomic scale cuts and stretching
2. **Forward simulation**: Calculate the frictional properties of the sheet using MD simulations
3. **Accelerated search**: Use machine learning to replace the MD simulations and perform an accelerated search for new designs

Main research question

Can we control the friction of a nanoscale Kirigami sheet with pattern design and straining of the sheet?

- Kirigami: Variation of origami with cuts permitted
- Desgins: Macroscale → nanoscale

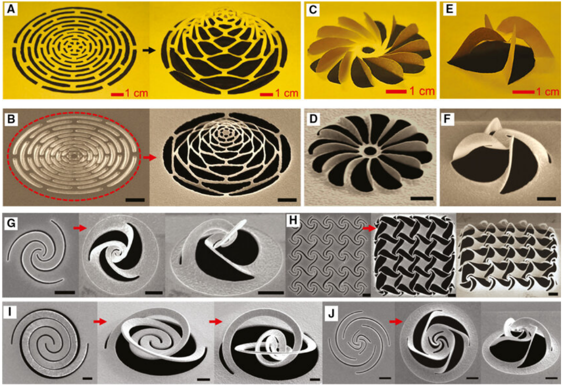

Figure: Example of macroscale Kirigami designs implemented on a microscale using a focused ion beam. Black scale bars: 1 μm. Reproduced from [1].

- Hanakata et al. [2, 3] found out-of-plane buckling with Kirigami designs
- Surface properties are predicted to be important for friction properties
  - Asperity theory: Contact area
  - Frenkel–Kontorova models: Commensurability

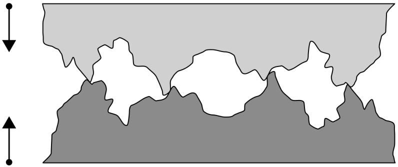

(a) Small load.

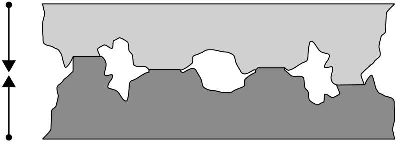

(b) High load.

Figure: Qualitatively illustration of the microscopic asperity deformation under increasing load. Reproduced from [4].

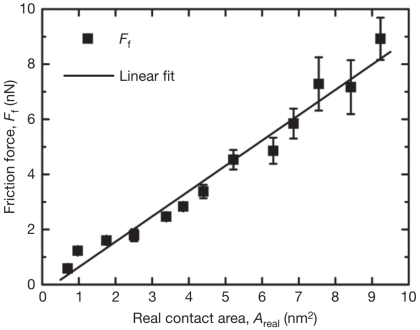

(a) Numerical MD results using an amorphous carbon tip and a diamond sample. Reproduced from [5] with permission from Springer Nature.

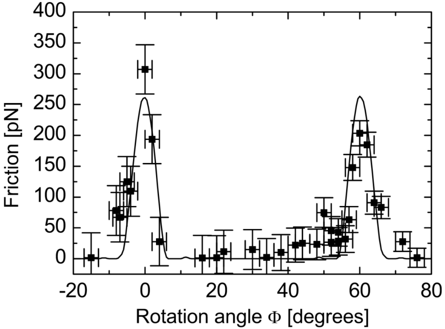

(b) Experimental results of a graphene sheet sliding on graphite. Adapted from [6], reproduced from [7] with permission from the American Physical Society.

Creating a graphene Kirigami system

System setup

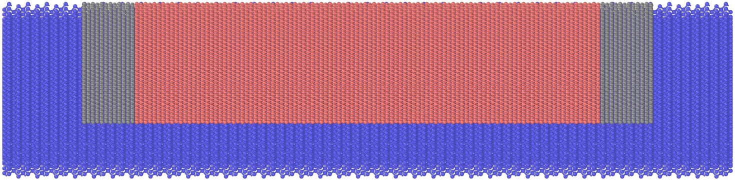

Figure: System of interest: Graphene sheet on a silicon substrate. Blue: Substrate, Red: Inner sheet, Grey: Pull blocks.

System setup

System size

$$\text{Atoms} \sim 60,000$$

$$\text{Sheet} \sim 130 \times 165$$

Regions

- Red: *NVE*
- Green: Thermostat *NVT*
- Blue: Rigid

(a) Side view.

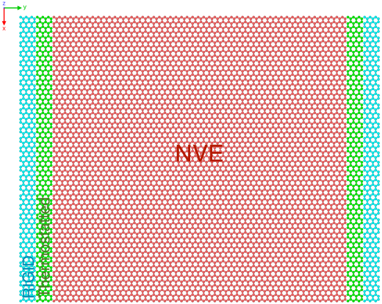

(b) Top view.

Sheet Kirigami

Indexing

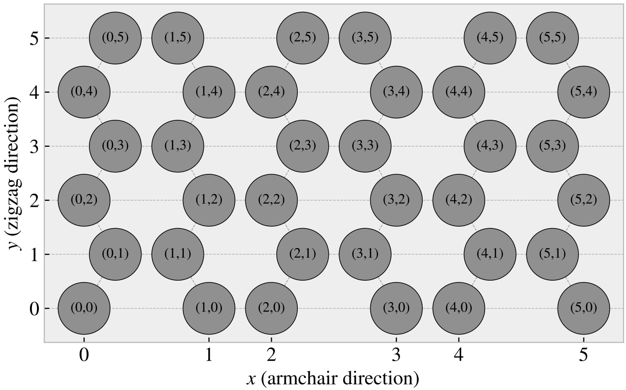

Figure: Graphene atom site indexing.

Sheet Kirigami
Indexing

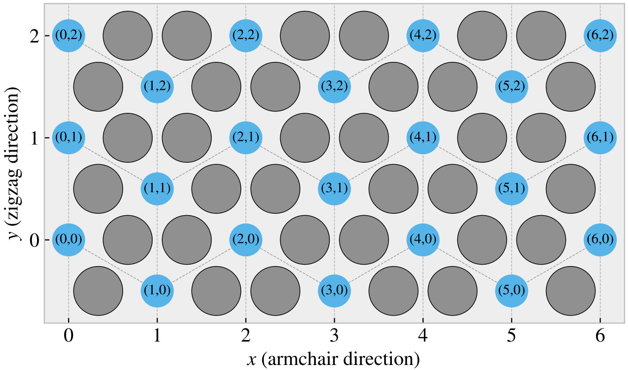

Figure: Graphene *center element* indexing.

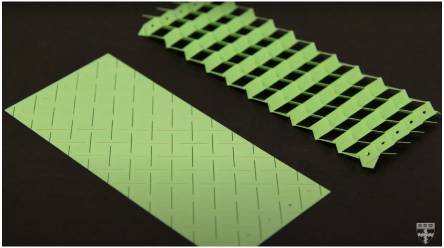

(a) Tetrahedron: Alternating perpendicular cuts producing a tetrahedron-shaped surface buckling when stretched. Reproduced from [8].

(b) Honeycomb: Scotch™ Cushion Lock™ [9] producing a honeycomb-shaped surface buckling when stretched. Reproduced from [9].

Figure: Macroscale kirigami cut patterns used as inspiration for the nanoscale implementation.

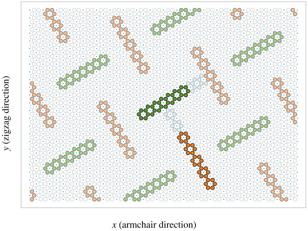
y (zigzag direction)
x (armchair direction)

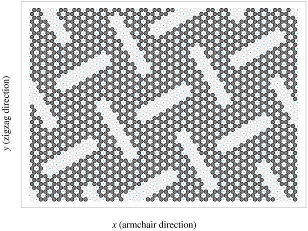
y (zigzag direction)
x (armchair direction)

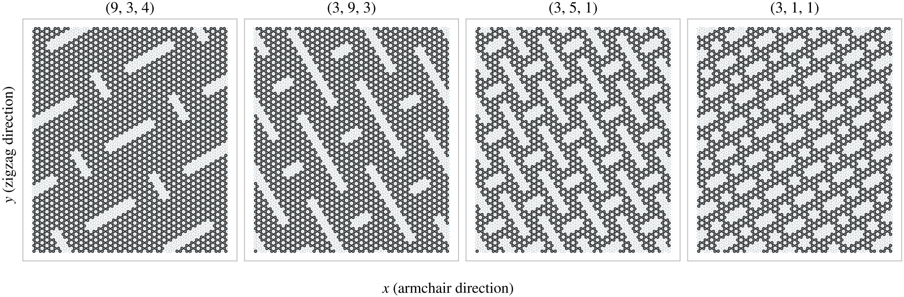
(9, 3, 4)
(3, 9, 3)
(3, 5, 1)
(3, 1, 1)
y (zigzag direction)
x (armchair direction)

Sheet Kirigami

Honeycomb patterns

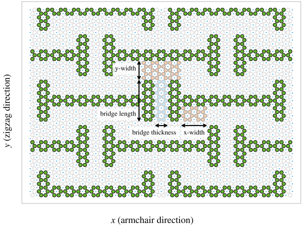

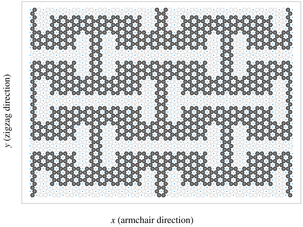

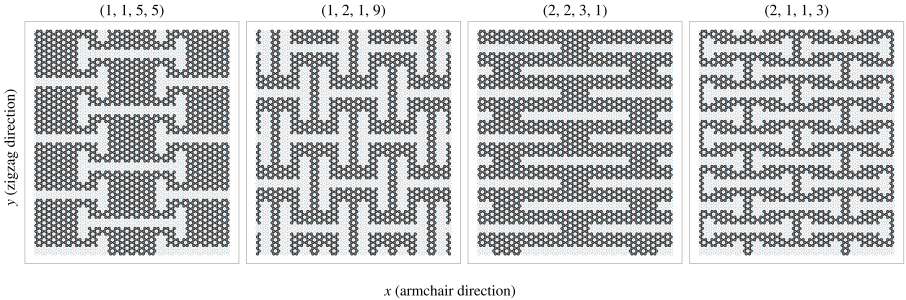

Sheet Kirigami
Random walk patterns

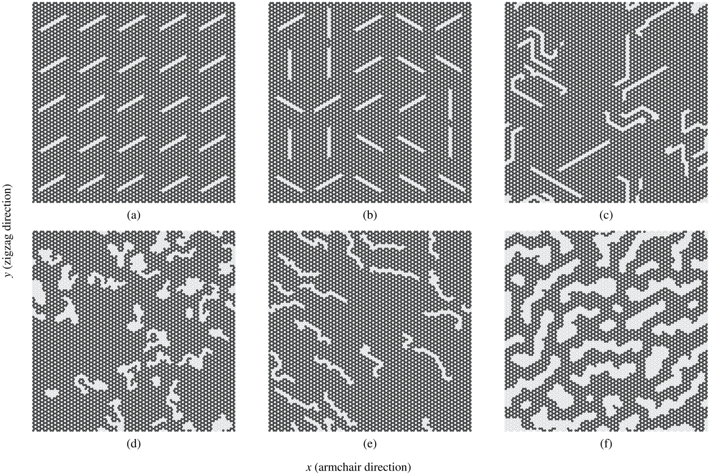

Molecular Dynamics (MD)

- Newtons equations (NVE)

$$m_i \frac{d^2 \mathrm{r}_i}{dt^2} = \mathrm{F}_i = -\nabla U_i,$$

- Introducing temperature (NVT) with the Langevin equation

$$m_i \frac{d^2 \mathrm{r}_i}{dt^2} = \underbrace{-\nabla U_i}_{F_i} \underbrace{-\alpha \mathrm{v}_i}_{\text{Drag}} + \underbrace{\mathrm{R}_i}_{\text{Fluctuation}},$$

$$\langle R \rangle = 0, \qquad \langle R^2 \rangle = 2\alpha k_B T.$$

Pilot study

Friction metrics

(a)
$K = \infty$,
$v = 20\ \frac{\mathbf{m}}{\mathbf{s}}$
(10 sliding).

(b)
$K = \infty$,
$v = 20\ \frac{\mathbf{m}}{\mathbf{s}}$
(100 sliding).

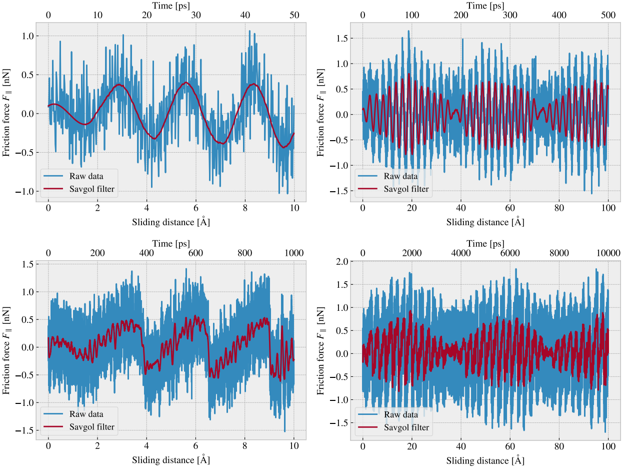

(c)
$K = 10\ \frac{\mathbf{N}}{\mathbf{m}}$,
$v = 1\ \frac{\mathbf{m}}{\mathbf{s}}$
(10 sliding).

(d)
$K = 10\ \frac{\mathbf{N}}{\mathbf{m}}$,
$v = 1\ \frac{\mathbf{m}}{\mathbf{s}}$
(100 sliding).

Figure: Friction force traces. The red line represents a Savgol filter.

Out-of-plane buckling

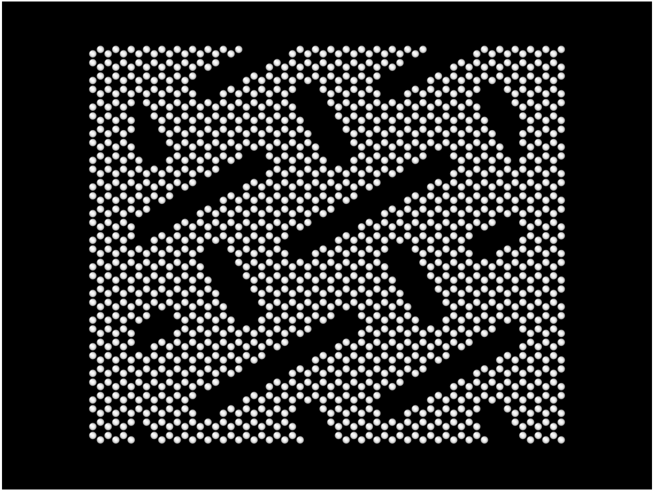

Figure: Kirigami sheet stretch in a vacuum.

Out-of-plane buckling

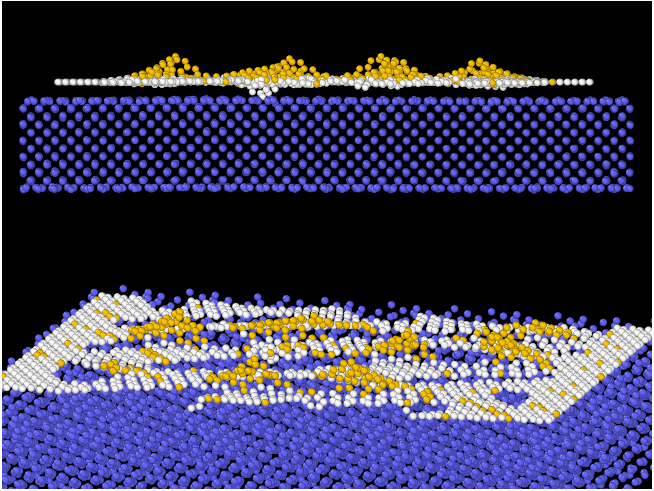

Figure: Kirigami stretch in contact with the substrate.

Out-of-plane buckling

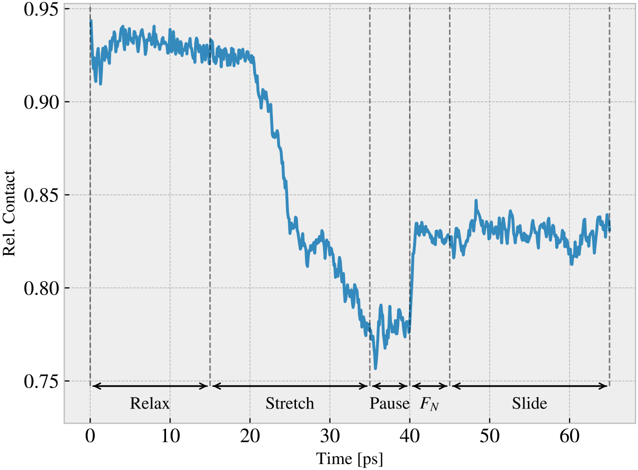

Figure: Contact area approximation: Number of C–Si bonds within a threshold distance of 110% the LJ interaction equilibrium distance.

Contact-strain profile

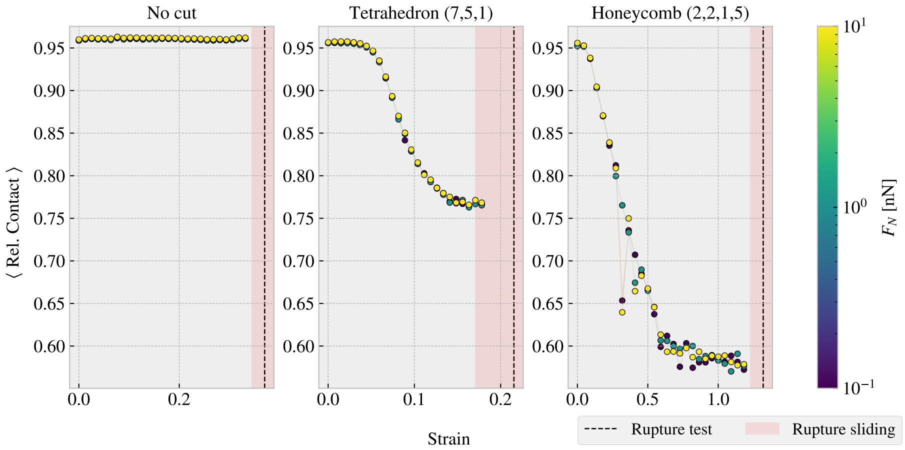

Figure: Contact-strain profile for $F_N = \{0.1, 1, 10\}$nN.

Friction-strain profile

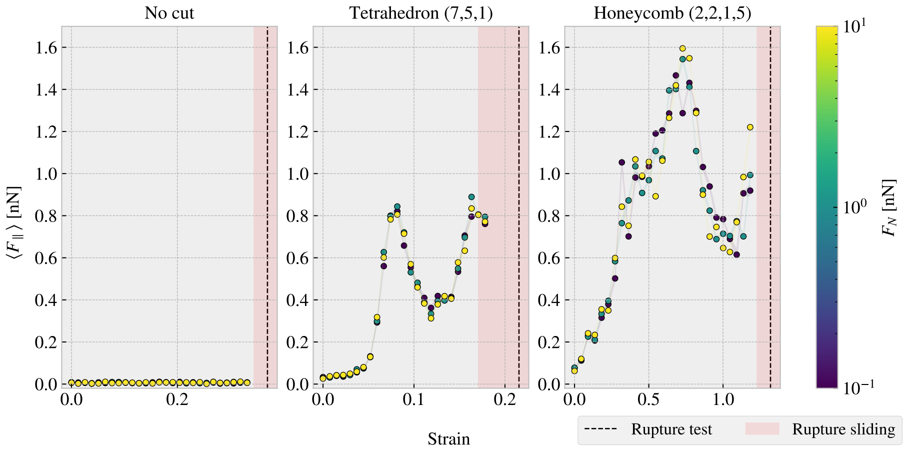

Figure: Friction-strain profile for $F_N = \{0.1, 1, 10\}$nN.

Negative friction coefficient

Coupling of load to sheet tension

$$F_t = TF_N, \qquad T = 6$$

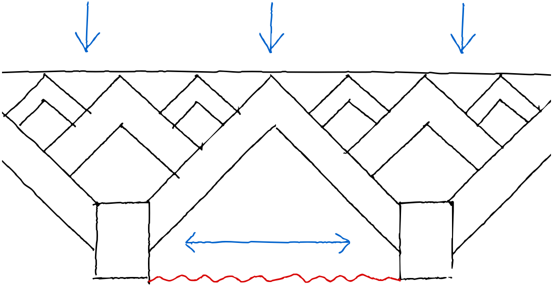

Figure: Working sketch for a nanomachine design translating applied load (from the top of the figure) to a straining of the graphene sheet (shown in red).

Negative friction coefficient

Tetrahedron results

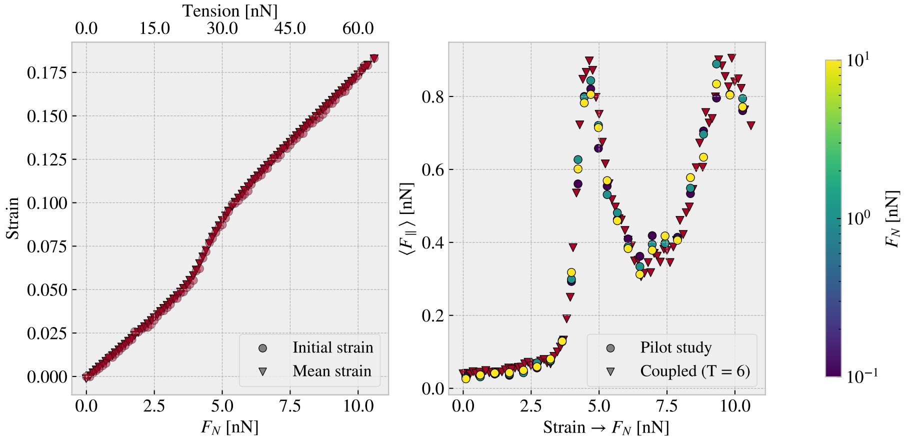

Figure: Tetrahedron $(7, 5, 1)$

Negative friction coefficient

Honeycomb results

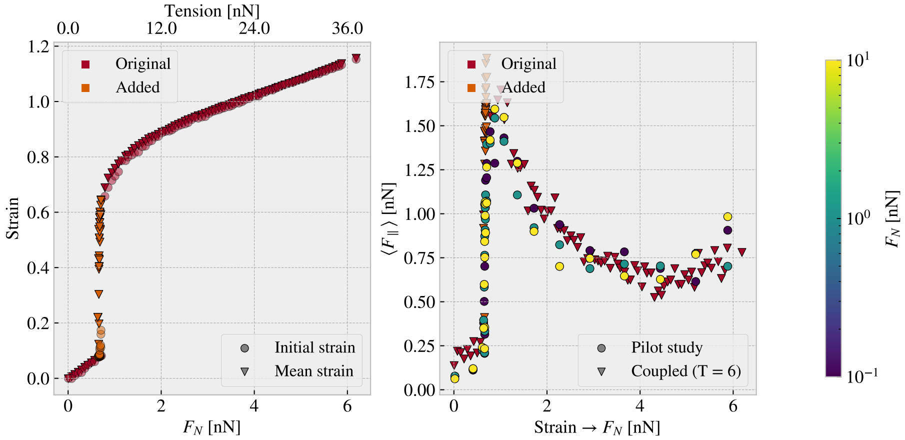

Figure: Honeycomb $(2, 2, 1, 5)$

Negative friction coefficient

Honeycomb deformations

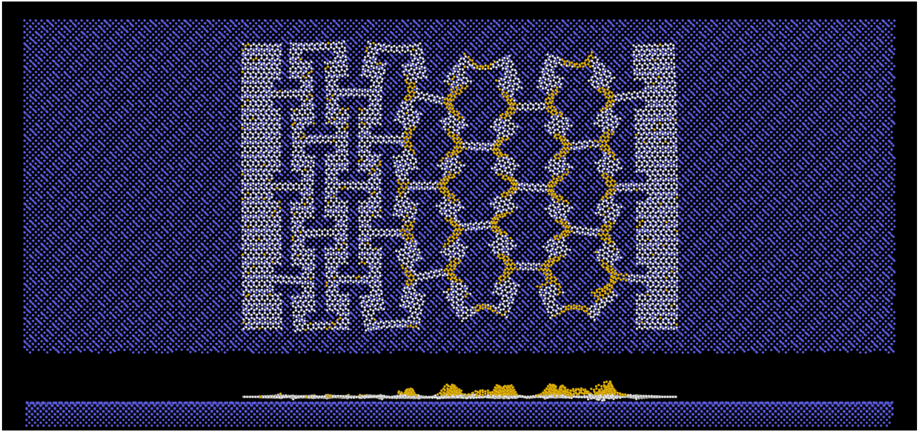

Figure: Honeycomb $(2, 2, 1, 5)$ stretch.

Kirigami configuration search

Dataset

Table: Summary of the generated data points in the dataset.

Type	Configurations	Data points	Ruptures
Pilot study	3	261	25 (9.58 %)
Tetrahedron	68	3015	391 (12.97 %)
Honeycomb	45	1983	80 (4.03 %)
Random walk	100	4401	622 (14.13 %)
Total	214 (216)	9660	1118 (11.57 %)

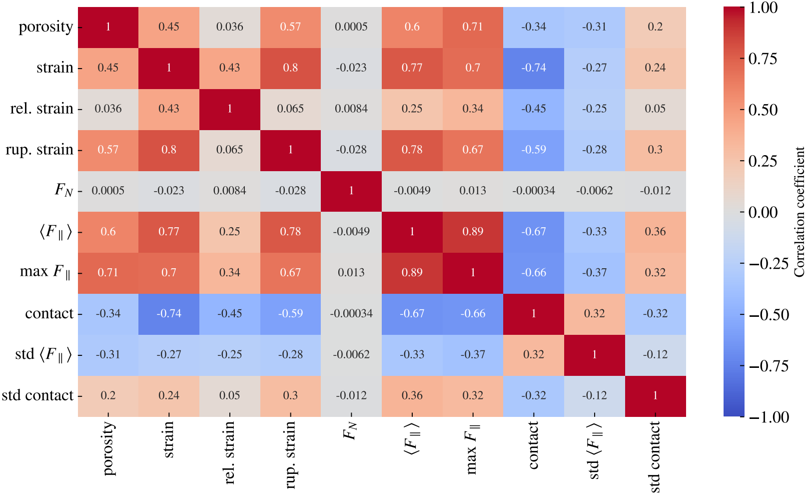

Figure: Pearson product-moment correlation coefficients.

Properties of interest

$$(1)\ \min F_{\text{fric}}, \qquad (2)\ \max F_{\text{fric}}, \qquad (3)\ \max \Delta F_{\text{fric}}, \qquad (4)\ \max \text{drop}.$$

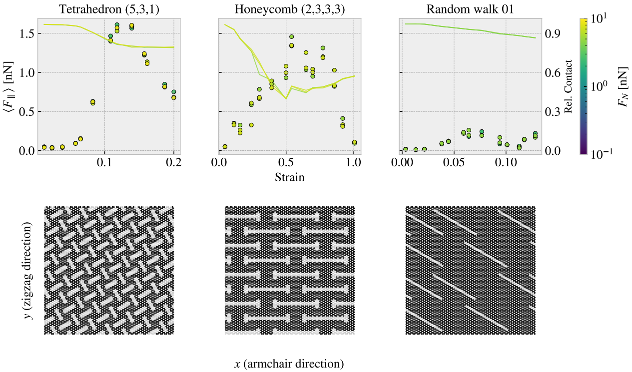

Figure: Max drop property. Best candidates in the dataset.

Machine learning

- Convolutional neural network
- Input: Kirigami configuration, strain and load
- Output: Mean friction, maximum friction, contact area, porosity, rupture, rupture strain

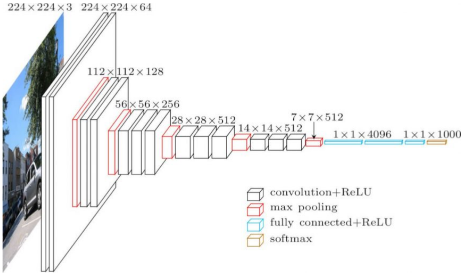

Figure: VGGNet-16 network convolutional network architecture. Reproduced from [10].

Table: Evaluation of the final model performance.

	R^2 [10^2]			Abs. [10^2]	Rel. [10^2]	Acc. [10^2]
	Mean F_f	Max F_f	Contact	Porosity	Rup. Strain	Rupture
Validation	98.067	93.558	94.598	2.325	12.958	96.102
Tetrahedron	88.662	85.836	64.683	1.207	5.880	99.762
Honeycomb	96.627	89.696	97.171	1.040	1.483	99.111

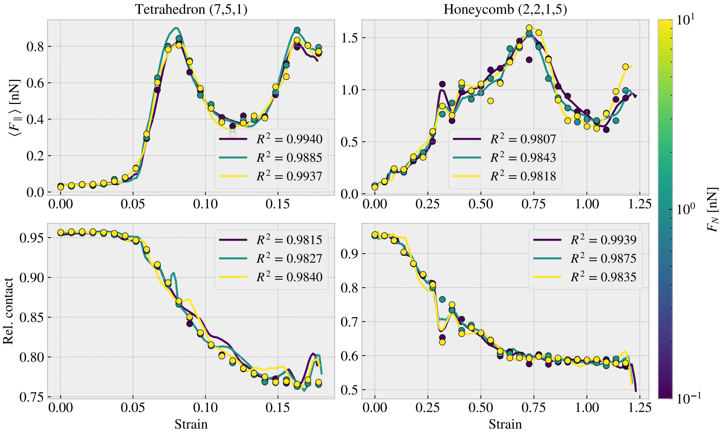

Figure: Visual evaluation of the final model predictions on the Tetrahedron $(7, 5, 1)$ and Honeycomb $(2, 2, 1, 5)$ used in the pilot study.

Accelerated search

Extended dataset

- Tetrahedron: 1.35×10^5 configurations
- Honeycomb: 2.025×10^6 configurations
- Random walk: 10^4 configurations

Search Pred.	Tetrahedron	Honeycomb	Random walk
min F_{fric}	-0.062	-0.109	-0.061
max F_{fric}	1.089	2.917	0.660
max ΔF_{fric}	1.062	2.081	0.629
max drop	0.277	1.250	0.269

Original	Tetrahedron	Honeycomb	Random walk
min F_{fric}	0.0067	0.0177	0.0024
max F_{fric}	1.5875	2.8903	0.5758
max ΔF_{fric}	1.5529	2.0234	0.5448
max drop	0.8841	1.2785	0.1818

Accelerated search
Random walk candidates

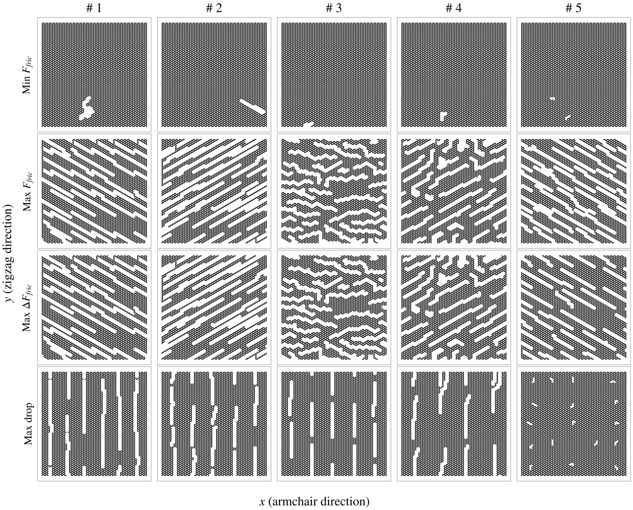

Figure: Top 5 candidates for the accelerated search using the Random walk generator.

Accelerated search

Translational variance

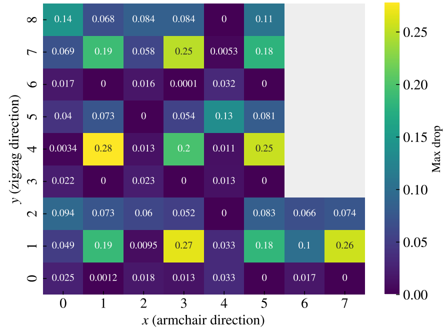

(a) Tetrahedron $(1, 7, 1)$. Rel. Std = 1.13

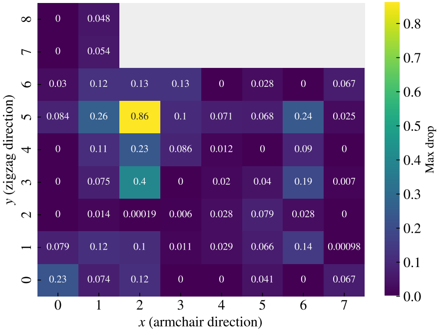

(b) Tetrahedron $(5, 3, 1)$. Rel. Std = 1.61

Figure: Machine learning prediction of the max drop property for all unique reference positions.

Genetic algorithm based on Markov chain probability.

1. Rank configurations by fitness score.
2. Calculate target states from the best candidates.
3. Assign a mutation probability based on ranking and target states the ranking.
4. Mutate and repeat.

Max drop property optimization $\rightarrow$ poor convergence

Accelerated search
Grad-CAM

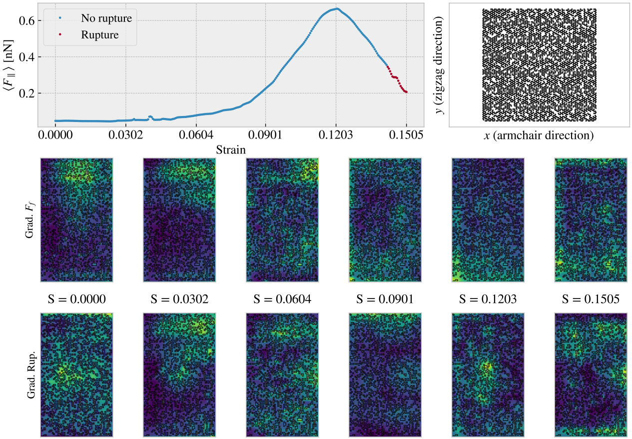

Figure: Genetic algorithm suggestion from a mixed porosity start. Top: Friction-strain curve and configuration. Bottom: Grad-CAM analysis

Grad-CAM

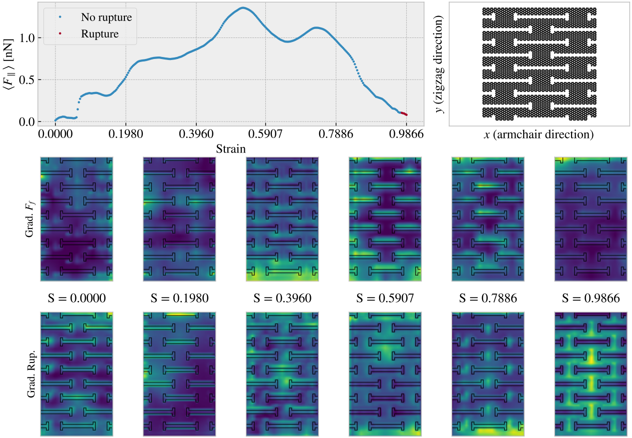

Figure: Honeycomb $(3, 3, 5, 3)$, ref $= (12, 0)$.

Outline

Summary and outlook

Key findings

- Non-monotonous relationship between friction and strain
- The coupled system can be exploited to achieve a negative friction coefficient
- Machine learning is feasible but more data is needed

Further studies:

- Investigation of the underlying mechanism
  - Commensurability hypothesis can be investigated by varying scan angle
- Friction-strain relationship at different physical conditions: temperature, sliding speed, spring stiffness.
- Edge and thermostat effects.
- Improve dataset with active learning

UiO : Department of Physics
University of Oslo

Mikkel Metzsch Jensen

Predicting Frictional Properties of Graphene Kirigami Using Molecular Dynamics and Neural Networks

References I

[1] J. Li and L. Zhiguang, "Focused-ion-beam-based nano-kirigami: from art to photonics", Nanophotonics **7**, 10.1515/nanoph-2018-0117 (2018).

[2] P. Z. Hanakata, E. D. Cubuk, D. K. Campbell, and H. S. Park, "Accelerated search and design of stretchable graphene kirigami using machine learning", Phys. Rev. Lett. **121**, 255304 (2018).

[3] P. Z. Hanakata, E. D. Cubuk, D. K. Campbell, and H. S. Park, "Forward and inverse design of kirigami via supervised autoencoder", Phys. Rev. Res. **2**, 042006 (2020).

[4] W. Commons, *File:asperities.svg — wikimedia commons, the free media repository*, (2023) https://commons.wikimedia.org/w/index.php?title=File:Asperities.svg&oldid=659167170 (visited on 02/03/2023).

[5] Y. Mo, K. T. Turner, and I. Szlufarska, "Friction laws at the nanoscale", Nature **457**, 1116–1119 (2009).

References II

[6] M. Dienwiebel, N. Pradeep, G. S. Verhoeven, H. W. Zandbergen, and J. W. Frenken, "Model experiments of superlubricity of graphite", Surface Science **576**, 197–211 (2005).

[7] A. Vanossi, N. Manini, M. Urbakh, S. Zapperi, and E. Tosatti, "Modeling friction: from nanoscale to mesoscale", Reviews of Modern Physics **85**, 529–552 (2013).

[8] L. Burrows, *New pop-up strategy inspired by cuts, not folds*, (Feb. 24, 2017) https://seas.harvard.edu/news/2017/02/new-pop-strategy-inspired-cuts-not-folds.

[9] *Scotch cushion lock protective wrap*, https://www.scotchbrand.com/3M/en_US/scotch-brand/products/catalog/~/Scotch-Cushion-Lock-Protective-Wrap/?N=4335+3288092498+3294529207&rt=rud.

[10] Neurohive, *VGG16 — Convolutional Network for Classification and Detection*, (2018) https://neurohive.io/en/popular-networks/vgg16/ (visited on 05/07/2023).